

## Reactivity of Cationic Molybdenum(II) Complexes. Part 2.<sup>1</sup> Electrochemical Reduction of the Eighteen-electron Complexes $[\text{Mo}(\text{CO})_3(\eta^5\text{-C}_5\text{Me}_5)\text{L}]^+$ [ $\text{L} = \text{CO}$ , $p\text{-MeC}_6\text{H}_4\text{NC}$ , or $\text{P}(\text{OMe})_3$ ]. Crystal Structure of $[\text{Mo}_2(\text{CO})_6(\eta^5\text{-C}_5\text{Me}_5)_2]^+$ \*

Piero Leoni

*Scuola Normale Superiore, Piazza dei Cavalieri, 7, 56100 Pisa, Italy*

Fabio Marchetti and Marco Pasquali

*Dipartimento di Chimica e Chimica Industriale dell' Università, Via Risorgimento, 35, 56100 Pisa, Italy*

Piero Zanello

*Dipartimento di Chimica dell' Università, Pian dei Mantellini, 44, 53100 Siena, Italy*

The 18-electron cationic complexes  $[\text{Mo}(\text{CO})_3(\eta^5\text{-C}_5\text{Me}_5)\text{L}]^+$  [ $\text{L} = \text{CO}$ ,  $p\text{-MeC}_6\text{H}_4\text{NC}$ , or  $\text{P}(\text{OMe})_3$ ] undergo, in dichloromethane solvent, a one-electron cathodic process, which gives rise to different products depending upon the nature of L. Through an e.c.c. electrode mechanism, the irreversible one-electron reduction of  $[\text{Mo}(\text{CO})_4(\eta^5\text{-C}_5\text{Me}_5)]^+$  and  $[\text{Mo}(\text{CO})_3(\eta^5\text{-C}_5\text{Me}_5)(p\text{-MeC}_6\text{H}_4\text{NC})]^+$  affords the dimer  $[\text{Mo}_2(\text{CO})_6(\eta^5\text{-C}_5\text{Me}_5)_2]$ , whereas  $[\text{Mo}(\text{CO})_3(\eta^5\text{-C}_5\text{Me}_5)\{\text{P}(\text{OMe})_3\}]^+$  leads to  $[\text{Mo}_2(\text{CO})_4(\eta^5\text{-C}_5\text{Me}_5)_2\{\text{P}(\text{OMe})_3\}_2]$ . The dimer  $[\text{Mo}_2(\text{CO})_6(\eta^5\text{-C}_5\text{Me}_5)_2]$  has been characterized by an X-ray structure determination. A preliminary electrochemical investigation on  $[\text{Mo}(\text{CO})(\eta^5\text{-C}_5\text{Me}_5)(\text{PhC}\equiv\text{CPh})_2]^+$  indicates that it can be reduced in two sequential one-electron quasi-reversible steps,  $[\text{Mo}(\text{CO})(\eta^5\text{-C}_5\text{Me}_5)(\text{PhC}\equiv\text{CPh})_2]$  and  $[\text{Mo}(\text{CO})(\eta^5\text{-C}_5\text{Me}_5)(\text{PhC}\equiv\text{CPh})]^-$  however being stable only for short times ( $t_{1/2} \approx 50$  s).

In Part 1<sup>1</sup> we dealt with the chemical reduction of 18-electron cationic molybdenum(II) complexes of general formula  $[\text{Mo}(\text{CO})_3(\eta^5\text{-C}_5\text{Me}_5)\text{L}]^+$ . The results obtained have shown that the reduction occurs at the strongly electrophilic metal. We present here an electrochemical study of the reduction processes of the species  $[\text{Mo}(\text{CO})_3(\eta^5\text{-C}_5\text{Me}_5)\text{L}]^+$  [ $\text{L} = \text{CO}$  (1),  $p\text{-MeC}_6\text{H}_4\text{NC}$  (2), or  $\text{P}(\text{OMe})_3$  (3)] in the hope that a comparison between chemical and electrochemical reductions may provide further information on the reactivity of such complexes. We note in addition that, despite the increasing interest towards molybdenum cyclopentadienyl-carbonyl complexes, their electrochemistry is almost unexplored.<sup>2,3</sup>

### Results and Discussion

**Electrochemistry.**—The cyclic voltammogram reported in Figure 1 shows that (1), in dichloromethane solution, undergoes one main reduction process. Controlled-potential coulometric experiments performed at potentials just beyond the cathodic peak A (working potential:  $-1.0$  V) led to the consumption of one mole of electrons per mole of (1). Cyclic voltammetry performed at scan rates varying from  $0.02$  V s<sup>-1</sup> to  $50$  V s<sup>-1</sup> indicated peak B, present in the reverse scan, to be attributable to the oxidation of fragmentation products of the one-electron reduced species rather than to direct reoxidation of the latter. In fact, the increase in scan rate results in peak B disappearing. Even at the highest scan rate ( $50$  V s<sup>-1</sup>), no directly associated reoxidation peak could be detected in the reverse scan after traversing peak A. Both the presence of the minor voltammetric responses B and C as a consequence of the cathodic step and the chemical evidence discussed below indicate that the electrochemical irreversibility of the one-electron reduction process is only apparent, being attributable to fast chemical reactions coupled to the charge transfer, rather than to any intrinsic

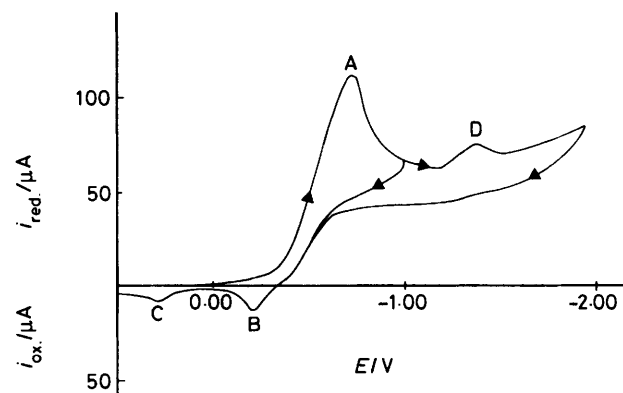


Figure 1. Cyclic voltammetric response recorded at a platinum electrode on a  $\text{CH}_2\text{Cl}_2$  solution containing (1) ( $3.6 \times 10^{-3}$  mol dm<sup>-3</sup>) and  $[\text{NBu}_4]\text{BF}_4$  (0.1 mol dm<sup>-3</sup>). Scan rate 0.2 V s<sup>-1</sup>

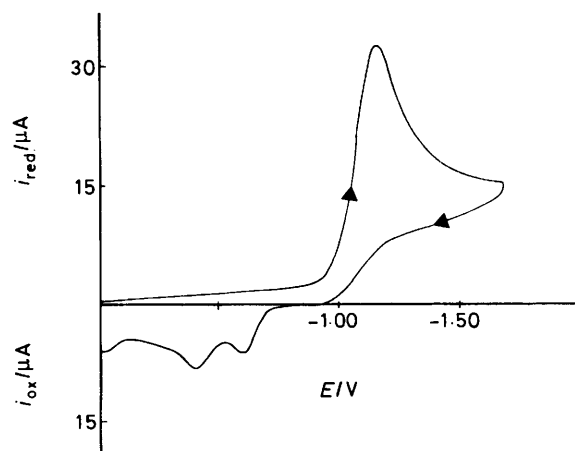


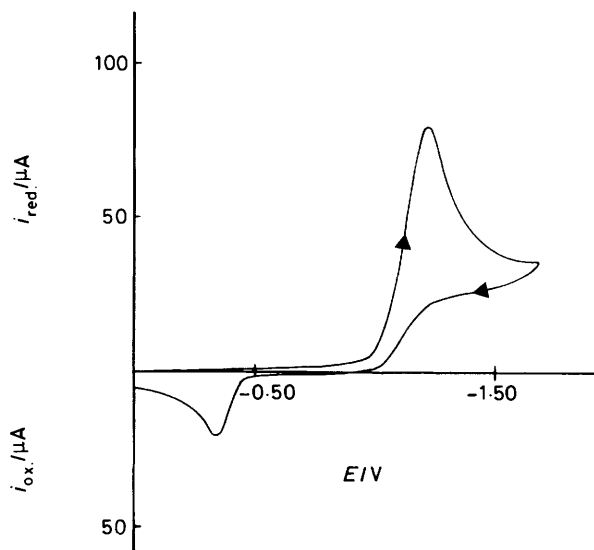
Figure 2. Cyclic voltammetric response recorded at a platinum electrode on a  $\text{CH}_2\text{Cl}_2$  solution containing (2) ( $9.6 \times 10^{-4}$  mol dm<sup>-3</sup>) and  $[\text{NBu}_4]\text{BF}_4$  (0.1 mol dm<sup>-3</sup>). Scan rate 0.2 V s<sup>-1</sup>

\* Bis[tricarbonyl(pentamethylcyclopentadienyl)molybdenum(II)].

Supplementary data available: see Instructions for Authors, *J. Chem. Soc., Dalton Trans.*, 1988, Issue 1, pp. xvii—xx.

**Table 1.** Potential values (V) of the redox changes recorded in dichloromethane solutions of  $[\text{Mo}_2(\text{CO})_6(\eta^5\text{-C}_5\text{H}_5)_2]$  and  $[\text{Mo}_2(\text{CO})_6(\eta^5\text{-C}_5\text{Me}_5)_2]$ . Peak potentials obtained at a scan rate of  $0.2 \text{ V s}^{-1}$  (CO ligands)

$\text{Mo}_2\text{L}_2$	$\text{Mo}_2\text{L}_2 + 2\text{e}^- \longrightarrow 2[\text{MoL}]^-$	$2[\text{MoL}]^- \longrightarrow \text{Mo}_2\text{L}_2 + 2\text{e}^-$	$\text{Mo}_2\text{L}_2 \longrightarrow 2[\text{MoL}]^+ + 2\text{e}^-$	$2[\text{MoL}]^+ + 2\text{e}^- \longrightarrow \text{Mo}_2\text{L}_2$
$[\text{Mo}_2(\text{CO})_6(\eta^5\text{-C}_5\text{H}_5)_2]$	-1.21	-0.09	+1.00	-0.42
$[\text{Mo}_2(\text{CO})_6(\eta^5\text{-C}_5\text{Me}_5)_2]$	-1.58	-0.22	+0.85	-0.51

**Figure 3.** Cyclic voltammogram recorded at a platinum electrode on a  $\text{CH}_2\text{Cl}_2$  solution containing (3) ( $2.3 \times 10^{-3} \text{ mol dm}^{-3}$ ) and  $[\text{NBu}_4]\text{BF}_4$  ( $0.1 \text{ mol dm}^{-3}$ ). Scan rate  $0.2 \text{ V s}^{-1}$ 

aspect of the interaction between reactant molecule and electrode surface.

Figure 2 shows that a qualitatively similar cyclic voltammetric behaviour holds for compound (2). In fact, apart from the different picture outlined by the reoxidation of short-lived intermediates arising from the reduction process, controlled-potential coulometry (working potential:  $-1.2 \text{ V}$ ) indicated that in this case also the reduction process involves a one-electron step. Also in this case no anodic peak directly associated with the cathodic process could be detected in the reverse scan even at  $50 \text{ V s}^{-1}$ . The solutions resulting from exhaustive cathodic electrolyses of (1) and (2) were examined in order to identify the electrogenerated products. In both cases, i.r. spectra in the terminal CO region displayed absorptions at  $2010$ ,  $1960$ ,  $1935$ ,  $1902$ ,  $1870$ , and  $1740 \text{ cm}^{-1}$ . Evaporation of the solvent, followed by extraction of the residue with toluene, afforded the dimer  $[\text{Mo}_2(\text{CO})_6(\eta^5\text{-C}_5\text{Me}_5)_2]$ , the X-ray structure of which was solved (see below).

While the electrochemical reduction of  $[\text{Mo}(\text{CO})_3(\eta^5\text{-C}_5\text{Me}_5)\text{L}]^+$  ( $\text{L} = \text{CO}$  or  $p\text{-MeC}_6\text{H}_4\text{NC}$ ) allows isolation of the dimer  $[\text{Mo}_2(\text{CO})_6(\eta^5\text{-C}_5\text{Me}_5)_2]$  in a pure form (ca. 60% yield), the literature method<sup>4</sup> for the synthesis of  $[\text{Mo}_2(\text{CO})_6(\eta^5\text{-C}_5\text{Me}_5)_2]$  is more laborious, chromatographic separation from  $[\text{Mo}_2(\text{CO})_4(\eta^5\text{-C}_5\text{Me}_5)_2]$  being necessary.<sup>4</sup>

The unexpected presence in solution of the absorptions at  $2010$ ,  $1960$ ,  $1870$ , and  $1740 \text{ cm}^{-1}$ , characteristic of  $[\text{Mo}(\text{CO})_3(\eta^5\text{-C}_5\text{Me}_5)]^+$  and  $[\text{Mo}(\text{CO})_3(\eta^5\text{-C}_5\text{Me}_5)]^-$ ,<sup>5</sup> in addition to those of the dimer ( $1935$  and  $1902 \text{ cm}^{-1}$ ),<sup>4</sup> was understood through the following experiment. The dimer  $[\text{Mo}_2(\text{CO})_6(\eta^5\text{-C}_5\text{Me}_5)_2]$  was dissolved in dichloromethane in the presence of an excess of  $[\text{NBu}_4]\text{BF}_4$ , used as supporting electrolyte in the electrochemical experiments. The resulting i.r.

**Table 2.** Peak potential values (V) for the one-electron reduction of  $[\text{Mo}(\text{CO})_3(\eta^5\text{-C}_5\text{Me}_5)\text{L}]^+$  in dichloromethane solution

L	$E_p^*$
CO	-0.73
$p\text{-MeC}_6\text{H}_4\text{NC}$	-1.17
$\text{P}(\text{OMe})_3$	-1.31

\* At a scan rate of  $0.2 \text{ V s}^{-1}$ .

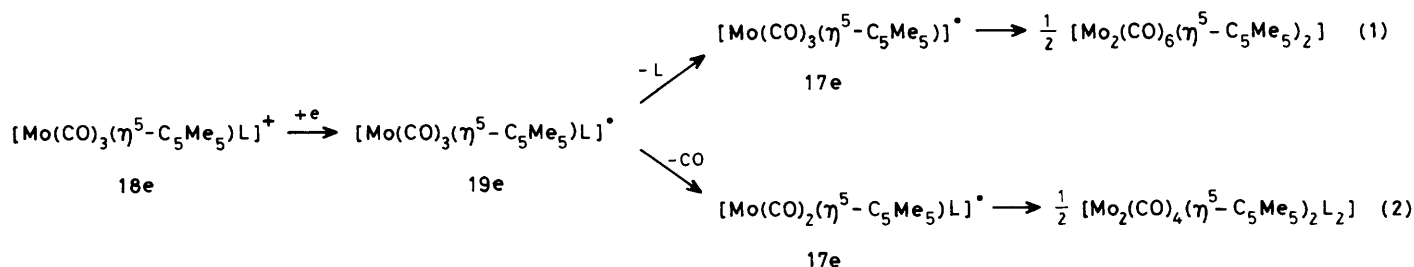
spectrum exhibited absorptions typical of  $[\text{Mo}_2(\text{CO})_6(\eta^5\text{-C}_5\text{Me}_5)_2]$ ,  $[\text{Mo}(\text{CO})_3(\eta^5\text{-C}_5\text{Me}_5)]^+$ , and  $[\text{Mo}(\text{CO})_3(\eta^5\text{-C}_5\text{Me}_5)]^-$ , indicating that the dimer undergoes a disproportionation reaction. The photochemical disproportionation of  $[\text{Mo}_2(\text{CO})_6(\eta^5\text{-C}_5\text{H}_5)_2]$  is known,<sup>6,7</sup> and has been reported to occur in the presence of salts possessing a co-ordinating anion,<sup>8</sup> as well as in the presence of a few Lewis bases.<sup>9-12</sup> The driving force for the reaction could be the achievement of an 18-electron closed-shell configuration by the cationic moiety. In this respect our results are somewhat different in that the disproportionation of the permethylated dimer is promoted by  $[\text{NBu}_4]\text{BF}_4$ , which contains only a weakly co-ordinating anion.

The electrochemical behaviour of  $[\text{Mo}_2(\text{CO})_6(\eta^5\text{-C}_5\text{H}_5)_2]$  has recently been elucidated.<sup>3</sup> In non-aqueous solvents it undergoes a two-electron oxidation as well as a two-electron reduction, both charge transfers being coupled to subsequent reactions. The compound  $[\text{Mo}_2(\text{CO})_6(\eta^5\text{-C}_5\text{Me}_5)_2]$  behaves in the same manner. Table 1 briefly compares the redox potentials of these steps for the two dimers, together with those of the products from the subsequent relevant chemical reactions. As expected the permethylated compound is more difficult to reduce and is more easily oxidized. In this light the ill-defined peak D in Figure 1 could be attributed to the cathodic reduction of the electrogenerated  $[\text{Mo}_2(\text{CO})_6(\eta^5\text{-C}_5\text{Me}_5)_2]$ .

Figure 3 illustrates the cyclic voltammetric behaviour of compound (3). As in the previous cases, a single one-electron reduction process is displayed, which does not show directly associated reoxidation processes in the reverse scan, even at the highest scan rate. The product resulting from exhaustive electrolysis was identified following the procedure reported above in the isolation of  $[\text{Mo}_2(\text{CO})_6(\eta^5\text{-C}_5\text{Me}_5)_2]$ . In this case  $[\text{Mo}_2(\text{CO})_4(\eta^5\text{-C}_5\text{Me}_5)_2\{\text{P}(\text{OMe})_3\}_2]$  was the recovered dimer, the identification being based on comparison of its spectroscopic properties with those of an authentic sample (see Experimental section). The result was not unexpected, since  $\text{P}(\text{OMe})_3$  is a very effective ligand for co-ordination to molybdenum in these systems.<sup>13</sup>

Table 2 summarizes the redox potentials for the reduction of the species (1)–(3). As expected, the greater the ability of L to increase the electronic density on the metal, the more cathodic the reduction potentials become.

In summary, the overall electrode mechanism involved in the cathodic reduction of the species (1)–(3) can be summarized according to different e.c.c. mechanisms, equations (1) and (2). In the case of  $\text{L} = \text{CO}$  or  $p\text{-MeC}_6\text{H}_4\text{NC}$  mechanism (1) is followed, whereas for  $\text{L} = \text{P}(\text{OMe})_3$  mechanism (2) holds. The formation and the evolution of 19-electron intermediates obtained by electrochemical reduction of 18-electron cations



has recently been discussed for carbonylmanganese(I) derivatives.<sup>14</sup>

We also wish to report here the results of a preliminary investigation on the cathodic behaviour of  $[\text{Mo}(\text{CO})(\eta^5\text{-C}_5\text{Me}_5)\text{L}_2]^+$  (**4**) ( $\text{L} = \text{PhC}\equiv\text{CPh}$ ). As shown in Figure 4, the alkyne derivative displays two sequential cathodic steps, with marked features of reversibility. Step by step controlled-potential coulometric experiments at the potentials of the two peaks indicated each of the two processes to involve one-electron per molecule. In addition, after exhaustive electrolyses, the species responsible for peaks C and D are no longer present.

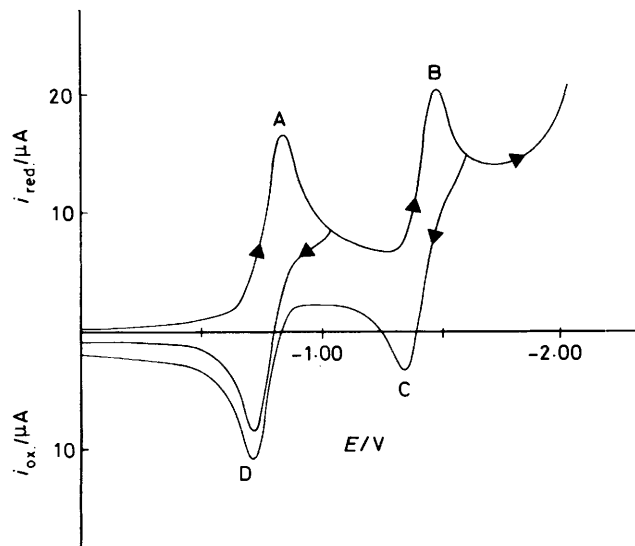


Figure 4. Cyclic voltammogram recorded at a platinum electrode on a  $\text{CH}_2\text{Cl}_2$  solution containing (**4**) ( $1.03 \times 10^{-3} \text{ mol dm}^{-3}$ ) and  $[\text{NBu}_4]\text{BF}_4$  ( $0.1 \text{ mol dm}^{-3}$ ). Scan rate  $0.2 \text{ V s}^{-1}$

Beyond any doubt these data indicate the occurrence of e.c. type cathodic processes, with the  $[\text{Mo}(\text{CO})(\eta^5\text{-C}_5\text{Me}_5)\text{L}_2]$  and  $[\text{Mo}(\text{CO})(\eta^5\text{-C}_5\text{Me}_5)\text{L}_2]^-$  species, electrogenerated in correspondence to the peaks A and B respectively, being unstable at longer electrolysis times.

Analysis of the cyclic voltammetric response A/D with the scan rate varying from  $0.02 \text{ V s}^{-1}$  to  $50 \text{ V s}^{-1}$  agrees with a quasi-reversible one-electron charge transfer complicated by subsequent chemical reactions ( $i_{pa}/i_{pc}$  increases from 0.86 at 0.02 to 1 at  $0.5 \text{ V s}^{-1}$ ;  $\Delta E_p$  increases from 75 at 0.02 to 620 mV at  $50 \text{ V s}^{-1}$ ;  $i_{pc}/v^{1/2}$  decreases by ca. 20%). The same features hold as far as the response B/C is concerned. At scan rates sufficient to prevent the chemical complications (*i.e.*, higher than  $0.5 \text{ V s}^{-1}$ ), it is possible to evaluate the following formal electrode potentials:  $E^{\circ'}\{[\text{Mo}(\text{CO})(\eta^5\text{-C}_5\text{Me}_5)\text{L}_2]^+ - [\text{Mo}(\text{CO})(\eta^5\text{-C}_5\text{Me}_5)\text{L}_2]\} = -0.77 \text{ V}$ ,  $E^{\circ'}\{[\text{Mo}(\text{CO})(\eta^5\text{-C}_5\text{Me}_5)\text{L}_2]^- - [\text{Mo}(\text{CO})(\eta^5\text{-C}_5\text{Me}_5)\text{L}_2]\} = -1.41 \text{ V}$ . In addition, assuming a first-order (or pseudo-first-order) reaction to be responsible for the instability of the species primarily generated at the electrode surface, it is possible to compute<sup>15</sup> a half-life of ca. 50 s for both  $[\text{Mo}(\text{CO})(\eta^5\text{-C}_5\text{Me}_5)\text{L}_2]$  and  $[\text{Mo}(\text{CO})(\eta^5\text{-C}_5\text{Me}_5)\text{L}_2]^-$  ( $\text{L} = \text{PhC}\equiv\text{CPh}$ ). Although further investigations are needed to identify the final products resulting from these cathodic processes, it is interesting to underline that both one- and two-electron reduction processes of  $[\text{Mo}(\text{CO})(\eta^5\text{-C}_5\text{Me}_5)(\text{PhC}\equiv\text{CPh})_2]^+$  do not cause immediate ligand losses. Diphenylacetylene molecules in  $[\text{Mo}(\text{CO})(\eta^5\text{-C}_5\text{Me}_5)(\text{PhC}\equiv\text{CPh})_2]^+$  act as three-electron ligands;<sup>16</sup> it is likely that the two one-electron steps correspond to the sequential conversion of the two acetylens into two-electron donors, so that molybdenum does not exceed the effective atomic number of 18; on the other hand the ability of acetylens to act as variable electron donors is well documented.<sup>17,18</sup> This behaviour does not contradict the main features of the electrochemical processes reported in the present paper; while the chemical reductions of  $[\text{Mo}(\text{CO})_3(\eta^5\text{-C}_5\text{Me}_5)\text{L}]^+$  species,<sup>1</sup>

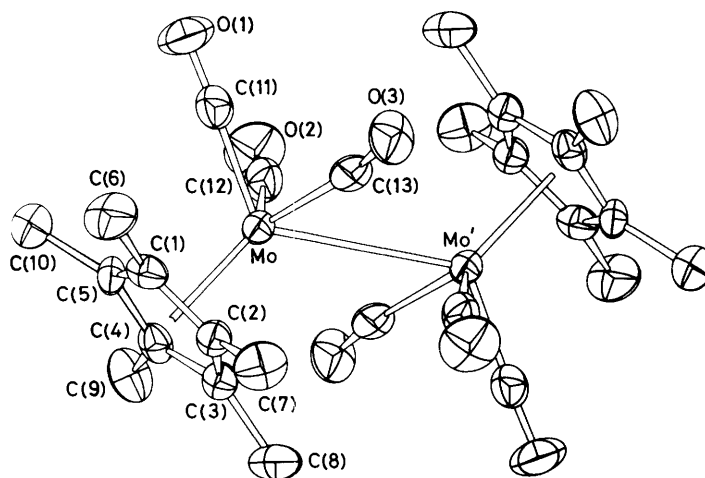


Figure 5. Molecular structure of  $[\text{Mo}_2(\text{CO})_6(\eta^5\text{-C}_5\text{Me}_5)_2]$

**Table 3.** Fractional co-ordinates ( $\times 10^4$ ) with estimated standard deviations in parentheses

Atom	X/a	Y/b	Z/c
Mo	1 367.8(6)	4 999.3(8)	6 003.4(3)
O(1)	1 846(6)	7 633(5)	7 230(4)
O(2)	2 515(7)	7 533(6)	5 187(4)
O(3)	-1 899(5)	5 400(5)	6 046(3)
C(1)	2 622(9)	3 591(7)	7 228(4)
C(2)	1 687(7)	2 595(8)	6 579(4)
C(3)	2 269(7)	2 545(7)	5 947(4)
C(4)	3 582(8)	3 517(7)	6 202(4)
C(5)	3 791(8)	4 150(7)	6 996(4)
C(6)	2 543(13)	3 844(9)	8 087(4)
C(7)	447(10)	1 582(9)	6 634(5)
C(8)	1 733(10)	1 481(8)	5 201(5)
C(9)	4 697(9)	3 654(9)	5 795(5)
C(10)	5 168(9)	5 101(12)	7 558(5)
C(11)	1 646(9)	6 648(8)	6 762(5)
C(12)	1 976(9)	6 590(8)	5 422(4)
C(13)	-785(8)	5 249(8)	5 936(4)

**Table 4.** Bond distances (Å) and angles ( $^\circ$ ), with estimated standard deviations in parentheses

Mo-C(1)	2.298(6)	O(3)-C(13)	1.148(10)
Mo-C(2)	2.365(7)	C(1)-C(2)	1.409(9)
Mo-C(3)	2.406(7)	C(1)-C(5)	1.414(12)
Mo-C(4)	2.376(8)	C(2)-C(3)	1.407(11)
Mo-C(5)	2.304(6)	C(3)-C(4)	1.424(9)
Mo-C(11)	1.927(8)	C(4)-C(5)	1.409(10)
Mo-C(12)	1.977(8)	C(1)-C(6)	1.521(12)
Mo-C(13)	1.987(8)	C(2)-C(7)	1.520(12)
Mo-cp	2.020(7)	C(3)-C(8)	1.506(10)
Mo-Mo'	3.278(4)	C(4)-C(9)	1.492(13)
O(1)-C(11)	1.163(10)	C(5)-C(10)	1.506(10)
O(2)-C(12)	1.154(11)		
C(11)-Mo-C(12)	77.5(3)	C(2)-C(3)-C(4)	108.5(6)
C(11)-Mo-C(13)	77.7(4)	C(3)-C(4)-C(5)	106.8(6)
C(12)-Mo-Mo'	74.8(2)	C(4)-C(5)-C(1)	108.9(6)
C(13)-Mo-Mo'	67.9(2)	C(5)-C(1)-C(2)	107.7(6)
C(11)-Mo-Mo'	121.4(2)	C(5)-C(1)-C(6)	125.9(7)
C(12)-Mo-C(13)	113.3(3)	C(6)-C(1)-C(2)	125.8(7)
C(11)-Mo-cp	113.7(3)	C(1)-C(2)-C(7)	125.0(6)
C(12)-Mo-cp	123.0(4)	C(7)-C(2)-C(3)	126.3(6)
C(13)-Mo-cp	123.7(3)	C(2)-C(3)-C(8)	125.0(7)
Mo'-Mo-cp	124.8(2)	C(8)-C(3)-C(4)	125.9(7)
Mo-C(11)-O(1)	178.6(8)	C(3)-C(4)-C(9)	126.7(6)
Mo-C(12)-O(2)	170.6(6)	C(9)-C(4)-C(5)	125.7(7)
Mo-C(13)-O(3)	168.5(6)	C(4)-C(5)-C(10)	124.9(7)
C(1)-C(2)-C(3)	108.1(6)		

Prime indicates position,  $-x$ ,  $1-y$ ,  $1-z$ . cp is the centre of the cyclopentadienyl ring.

being ligand centred, do not alter either the oxidation state or the effective atomic number of molybdenum, the electrochemical reductions are metal centred and when the effective atomic number, 18, is exceeded a fast dissociative step takes place.

**X-Ray Structure of  $[\text{Mo}_2(\text{CO})_6(\eta^5\text{-C}_5\text{Me}_5)_2]$ .**—The crystal structure of  $[\text{Mo}_2(\text{CO})_6(\eta^5\text{-C}_5\text{Me}_5)_2]$  is shown in Figure 5. The co-ordinates of the non-hydrogen atoms are listed in Table 3, and bond distances and angles are collected in Table 4. The molecular structure of  $[\text{Mo}_2(\text{CO})_6(\eta^5\text{-C}_5\text{Me}_5)_2]$  compares very well with that of analogous  $[\text{M}_2(\text{CO})_6(\eta^5\text{-C}_5\text{H}_5)_2]$  compounds ( $\text{M} = \text{Cr}, \text{Mo}, \text{or W}$ ).<sup>19</sup> The two moieties of the molecule in the unit cell are related only by the inversion centre. However, the arrangement approximately displays two other elements of symmetry: (i) a mirror plane passing through the

**Table 5.** Experimental data for the crystallographic analysis\*

Compound	$[\text{Mo}_2(\text{CO})_6(\eta^5\text{-C}_5\text{Me}_5)_2]$
Formula	$\text{C}_{13}\text{H}_{15}\text{MoO}_3$
M	315.2
Space group	$P2_1/c$
a/Å	9.389(8)
b/Å	9.104(4)
c/Å	17.112(10)
$\beta/^\circ$	115.68(8)
$U/\text{Å}^3$	1 318(2)
Z	2
$D_s/\text{g cm}^{-3}$	1.588
F(000)	636
Temperature/K	295
Crystal size/mm	$0.20 \times 0.28 \times 0.45$
Diffraction	Ital Structures
$\mu/\text{mm}^{-1}$	0.964
Scan speed/ $^\circ \text{s}^{-1}$	0.1 (in $\omega$ )
Scan width/ $^\circ$	1.20 (in $\omega$ )
Radiation	Mo- $K_\alpha$
$\theta$ range/ $^\circ$	3–25
h range	0–12
k range	$\bar{1}$ –12
l range	$\bar{1}$ –18
Standard reflection	311
Intensity variation	None
Scan mode	$\theta/2\theta$
No. of measured reflections	3 680
Condition for observed reflections	$F_o > 3\sigma(F_o)$
No. of reflections used in the refinement	1 346
$R_{\text{int}} = \left\{ \frac{\sum [N \sum w(\langle F \rangle - F)]^2}{\sum [(N-1) \sum w F^2]} \right\}^{\frac{1}{2}}$	0.0220
Max. shift to error ratio	0.4
Min. max. height in final $\Delta\rho/e \text{ Å}^{-3}$	-0.7, 0.4
No. of refined parameters	169
$R = \sum  \Delta F  / \sum F_o$	0.0371
$R' =  \sum w(\Delta F)^2 / \sum w F_o^2 ^{\frac{1}{2}}$	0.0328
$S =  \sum w(\Delta F)^2 / (N - P) ^{\frac{1}{2}}$	2.69
w	$1/[\sigma^2(F_o) + 0.000 095 F_o^2]$

\*  $N$  = Number of observations,  $P$  = number of parameters.

molybdenum atoms and the centres of the cyclopentadienyl rings, (ii) a perpendicular two-fold axis, with a resulting approximate site symmetry  $2/m$  ( $C_{2h}$ ). The co-ordination polyhedron around molybdenum could be described as a distorted square pyramid having the base on C(11), C(12), C(13), and the symmetry related Mo atom, and the vertex on the centre of the cyclopentadienyl ring. The major cause of distortion in the pyramid is related to the large difference between Mo-CO and Mo-Mo' distances.

The Mo-Mo' distance of 3.278 Å, which is significantly longer than that observed in  $[\text{Mo}_2(\text{CO})_6(\eta^5\text{-C}_5\text{H}_5)_2]$  (3.235 Å),<sup>19</sup> is likely to be affected by the difference in hindrance between  $\text{C}_5\text{H}_5$  and  $\text{C}_5\text{Me}_5$ . The cyclopentadienyl rings are planar as could be expected, and the methyl groups lie just out of the plane (0.17–0.20 Å) on the opposite side relative to molybdenum.

The average Mo-CO distance of 1.964 Å is not significantly shorter than the 1.977 Å observed in  $[\text{Mo}_2(\text{CO})_6(\eta^5\text{-C}_5\text{H}_5)_2]$ , but in our case there is a larger dispersion in the distances. In both cases however, the shortest Mo-CO distance corresponds to the carbonyl group lying on the approximate symmetry plane and the related Mo-C-O bond angle is the nearest to  $180^\circ$ .

## Experimental

All preparations were carried out under an atmosphere of purified nitrogen; solvents were dried and purified by reflux over a suitable drying agent and distilled under nitrogen.

*Synthesis of the Complexes.*—The complexes  $[\text{Mo}(\text{CO})_3(\eta^5\text{-C}_5\text{Me}_5)\text{L}]\text{BF}_4$  [ $\text{L} = \text{CO}$ ,  $p\text{-MeC}_6\text{H}_4\text{NC}$ , or  $\text{P}(\text{OMe})_3$ ] were prepared as previously reported.<sup>1</sup>

$[\text{Mo}(\text{CO})(\eta^5\text{-C}_5\text{Me}_5)(\text{PhC}\equiv\text{CPh})_2]\text{BF}_4$ .  $[\text{Mo}(\text{CO})_3(\eta^5\text{-C}_5\text{Me}_5)]\text{BF}_4$  (1.264 g, 3.14 mmol) dissolved in  $\text{CH}_2\text{Cl}_2$  (10  $\text{cm}^3$ ) was added dropwise at  $-30^\circ\text{C}$  to a solution containing  $\text{PhC}\equiv\text{CPh}$  (1.339 g, 7.51 mmol) in  $\text{CH}_2\text{Cl}_2$  (5  $\text{cm}^3$ ). The temperature of the red solution obtained was raised to room temperature and diethyl ether (50  $\text{cm}^3$ ) was added. A yellow microcrystalline solid started to precipitate; by cooling at  $-78^\circ\text{C}$  for 2 h, the amount of yellow solid increased. The solid was filtered off, washed with diethyl ether, and vacuum dried; yield 1.609 g (2.29 mmol, 72.8%) (Found: C, 66.5; H, 4.6. Calc. for  $\text{C}_{39}\text{H}_{35}\text{BF}_4\text{MoO}$ : C, 66.7; H, 5.0%). I.r. (Nujol)  $\nu(\text{C}-\text{O})$  2 040 vs  $\text{cm}^{-1}$ .  $^1\text{H}$  N.m.r. ( $\text{CDCl}_3$ ,  $\text{SiMe}_4$ ):  $\delta$  2.0 (s, 15 H,  $\text{C}_5\text{Me}_5$ ), and 7.2–7.9 (m, 20 H,  $\text{C}_6\text{H}_5$ ).

$[\text{Mo}_2(\text{CO})_4(\eta^5\text{-C}_5\text{Me}_5)_2\{\text{P}(\text{OMe})_3\}_2]$ . To a solution containing  $[\text{Mo}_2(\text{CO})_6(\eta^5\text{-C}_5\text{Me}_5)_2]$  in toluene (20  $\text{cm}^3$ ) an excess of  $\text{P}(\text{OMe})_3$  (0.4 g) was added. The resulting suspension was refluxed for 24 h. An orange-yellow solution formed, from which  $[\text{Mo}_2(\text{CO})_4(\eta^5\text{-C}_5\text{Me}_5)_2\{\text{P}(\text{OMe})_3\}_2]$  was obtained as a yellow solid in 20% yield after column chromatography ( $\text{CHCl}_3$  eluant; silica gel column). I.r. (Nujol)  $\nu(\text{C}-\text{O})$  1 940s, 1 860s  $\text{cm}^{-1}$ .  $^1\text{H}$  N.m.r. ( $\text{CDCl}_3$ ,  $\text{SiMe}_4$ ):  $\delta$  1.96 (s br, 30 H,  $\text{C}_5\text{Me}_5$ ), 3.67 [d, 9 H,  $\text{P}(\text{OMe})_3$ ], and 3.77 [d, 9 H,  $\text{P}(\text{OMe})_3$ ].

*X-Ray Data Collection.*—The relevant details of crystal parameters, data collection, and structure refinement for  $[\text{Mo}_2(\text{CO})_6(\eta^5\text{-C}_5\text{Me}_5)_2]$  are summarized in Table 5. The unit-cell dimensions were determined by least-squares fitting of the  $\theta$  angles of 24 intense reflections chosen from diverse regions of reciprocal space in the  $11\text{--}15^\circ$   $\theta$  range. The reflection intensities were corrected for Lorentz and polarization effects. The structure was solved by Patterson and Fourier techniques and refined by the full-matrix least-squares method using the SHELX 76 program.<sup>20</sup> Twelve of the fifteen hydrogen atoms were located from a difference Fourier synthesis. The remainder were introduced in calculated positions; the positional parameters of hydrogens were not refined. Atomic scattering factors and anomalous scattering coefficients were taken from the literature.<sup>21</sup> Calculations were carried out on the IBM 3081/K computer of the Centro Nazionale Universitario di Calcolo Elettronico, C.N.R., Pisa. PARST<sup>22</sup> and ORTEP<sup>23</sup> programs were used for the geometrical calculations and structure drawing.

*Electrochemistry.*—Both the materials and the apparatus used in the electrochemical tests have been described elsewhere.<sup>24</sup> Potential values refer to a saturated aqueous calomel electrode (s.c.e.). Under the present experimental con-

ditions, in dichloromethane solution the  $[\text{Fe}(\eta^5\text{-C}_5\text{H}_5)_2]^+ - [\text{Fe}(\eta^5\text{-C}_5\text{H}_5)_2]$  couple is located at +0.49 V. The temperature was controlled at  $20 \pm 0.1^\circ\text{C}$ .

### Acknowledgements

We gratefully thank Dr. M. Pasero for help in collection of the intensity data, and the Ministry of Education for financial support.

### References

- 1 P. Leoni, E. Aquilini, M. Pasquali, F. Marchetti, and M. Sabat, *J. Chem. Soc., Dalton Trans.*, 1988, 329.
- 2 W. E. Geiger, P. H. Rieger, B. Tulyathan, and M. D. Rausch, *J. Am. Chem. Soc.*, 1984, **106**, 7000.
- 3 K. M. Kadish, D. A. Lacombe, and J. E. Anderson, *Inorg. Chem.*, 1986, **25**, 2246.
- 4 D. S. Ginley and M. S. Wrighton, *J. Am. Chem. Soc.*, 1975, **97**, 3533.
- 5 P. Leoni, E. Grilli, M. Pasquali, and M. Tomassini, *J. Chem. Soc., Dalton Trans.*, 1986, 1041.
- 6 T. J. Meyer and J. V. Caspar, *Chem. Rev.*, 1985, **85**, 4434.
- 7 C. E. Philbin, A. S. Goldman, and D. R. Tyler, *Inorg. Chem.*, 1986, **25**, 4434.
- 8 A. E. Stiegman and D. R. Tyler, *J. Am. Chem. Soc.*, 1985, **107**, 967.
- 9 R. J. Haines, R. S. Nyholm, and M. H. B. Stiddard, *J. Chem. Soc. A*, 1968, 43.
- 10 R. B. King, K. H. Pannel, C. A. Eggers, and L. W. Houk, *Inorg. Chem.*, 1968, **7**, 2353.
- 11 R. J. Haines and C. R. Nolte, *J. Organomet. Chem.*, 1970, **24**, 725.
- 12 P. Hackett, P. S. O'Neill, and A. R. Manning, *J. Chem. Soc., Dalton Trans.*, 1974, 1625.
- 13 D. J. Darensbourg, *Adv. Organomet. Chem.*, 1982, **21**, 113.
- 14 D. J. Kuchynka, C. Amatore, and J. K. Kochi, *Inorg. Chem.*, 1986, **25**, 4087.
- 15 R. S. Nicholson and I. Shain, *Anal. Chem.*, 1964, **36**, 706.
- 16 K. A. Mead, H. Morgan, and P. Woodward, *J. Chem. Soc., Dalton Trans.*, 1983, 271.
- 17 B. Capelle, A. L. Beauchamp, M. Dartiguenave, and Y. Dartiguenave, *J. Chem. Soc., Chem. Commun.*, 1982, 366.
- 18 J. L. Davidson and G. Vasapollo, *J. Chem. Soc., Dalton Trans.*, 1985, 2239.
- 19 R. D. Adams, D. M. Collins, and F. A. Cotton, *Inorg. Chem.*, 1974, **13**, 1086.
- 20 G. M. Sheldrick, SHELX 76, Program for Crystal Structure Determinations, University of Cambridge, 1976.
- 21 'International Tables for X-Ray Crystallography,' Kynoch Press, Birmingham, 1974, vol. 4.
- 22 M. Nardelli, *Comput. Chem.*, 1983, **7**, 95.
- 23 C. K. Johnson, ORTEP, Report ORNL 3794, Oak Ridge National Laboratory, Tennessee, 1965.
- 24 F. Cecconi, C. A. Ghilardi, S. Midollini, A. Orlandini, and P. Zanello, *Polyhedron*, 1986, **5**, 2021.

Received 2nd March 1987; Paper 7/382